

# Thin Ribbon Tapered Coupler for Dielectric Waveguide/Optical Fiber†

C. Yeh \* and T. Y. Otoshi  
Jet Propulsion Laboratory  
California Institute of Technology  
Pasadena, CA 91109

F. I. Shimabukuro  
Aerospace Corporation  
P.O. Box 92957  
Los Angeles, CA 90009

## Abstract

The traditional tapered-to-a-point coupler for dielectric rod waveguide, and even the new cusp-like end termination for a single-mode optical fiber, fail when the dielectric constant of the dielectric waveguide is large. This paper presents a new way to design a low-loss coupler for high- or low-dielectric constant, dielectric waveguide for optical or millimeter/submillimeter waves.

---

†The research described in this publication was partly supported by the Jet Propulsion Laboratory, California Institute of Technology, under a contract with the National Aeronautics and Space Administration, and partly supported by a contract with the U.S. Air Force.

\*Consultant to JPL.

## Introduction

A recent discovery that high-dielectric constant, low-loss, solid dielectric material, such as *TiO* ( $\epsilon_1/\epsilon_0 = 100$ ,  $\tan \delta = 0.00025$ ) or *Rexolite* ( $\epsilon_1/\epsilon_0 = 2.55$ ,  $\tan \delta = 0.001$ ), can be made into a ribbon-like waveguide structure to yield an attenuation constant of less than 20 dB/km for single-mode guidance of millimeter/submillimeter waves,<sup>1</sup> provides the impetus to perfect a practical low-loss guided transmission system for these short wavelengths.<sup>2</sup> One of the crucial components which must be invented in order to guarantee the low-loss characteristics of this dielectric waveguide guiding system is the excitation coupler. One conventional way to minimize the coupling loss of an excitation coupler is by tapering the coupling end of a dielectric waveguide to a very narrow, sharp apex.<sup>3</sup> However, this method fails when the relative dielectric constant of the dielectric waveguide is much greater than unity, the free-space value. Another way is to shape the coupling end of an optical fiber waveguide into a cusp-like form.<sup>4</sup> This design, which is based on the direct application of geometrical optics to minimize reflection is applicable to guided wave structures whose cross-sectional dimensions are many free-space wavelengths. In the optical fiber case, the proximity of the dielectric constants of the core and cladding material enables the core diameter of a single-mode fiber to be as large as 20 free-space wavelengths, while that of a multi-mode fiber can be larger than 50 free-space wavelengths.

Neither of the above two techniques are applicable to the case of a dielectric waveguide with large dielectric constant difference between the core and cladding material and with a guide dimension less than the free-space wavelength, such as the ultra-low-loss millimeter/submillimeter dielectric ribbon waveguide.<sup>1</sup> This paper will describe a new low-loss coupler for this case.

## Impedance Matching Approach

It is possible to define a wave impedance for a given propagating mode along a dielectric waveguide of a given cross-sections. The wave impedance may be viewed as the characteristic impedance of a transmission line (i.e., the dielectric waveguide). Thus, a tapered (tapered in the direction of propagation of the guided wave, the z-direction) dielectric waveguide is then viewed as an inhomogeneous transmission line with z-dependent characteristic impedance.<sup>6</sup> The problem of designing a transition between a dielectric waveguide and free space becomes one of impedance matching the characteristic impedance of a given dielectric waveguide mode to the characteristic impedance (377 ohms) of free space. It is known that, between two transmission lines with different characteristic impedances, best matching can be achieved over a broadband of frequencies with a tapered section of transmission line.<sup>7,8</sup> For this reason, in practice, transitions between dielectric waveguide and free space, are generally of the tapered transmission line type. The shape of the taper is based upon one that produces the minimum mismatch losses over the frequency band of interest.

In principle, this tapering approach to a narrowed thin apex is workable for any dielectric waveguide with any dielectric constant. In practice, however, this approach is only workable for dielectric waveguide with a relative dielectric constant near unity. This is because when the core dielectric constant is large, to achieve good matching with free space, the tapered section must be very, very long and the cross-sectional dimension of the taper must be very small, making the tapered section extremely difficult to handle and align. The stability of the modal field to adhere to the tapered guiding section also becomes questionable. In other words, it is difficult to excite a guided wave along this type of tapered

section for a high dielectric constant guide, even though good impedance matching is present. It appears that the surface area for this high dielectric constant tapered section is too small to capture the incident wave and to transform it to a guided wave.’

### **Ribbon Transition Approach**

**The** remedy appears to be quite clear. For a high-dielectric constant guide, instead of tapering the guide to a very small cross-sectional area, the guide should be flattened to a large surface area and very thin thickness; <sup>1</sup> i.e., the transition region should be tapered to a thin, flat, but wide ribbon as shown in Fig. 1. To provide further improvements in matching, the end of the transition region can be further extended with a comb-like structure as shown in Fig. 2. Because of the large surface area of this structure, it can be easily supported mechanically without causing noticeable interference to the electromagnetic field. The large surface area also enables the guided surface wave to better attach to the guiding structure, thus improving the launching efficiency. <sup>1</sup>

It can be seen from Fig. 2 that this ribbon transition region is very different than the conventional tapered-to-a-point transition region used by all earlier investigators to obtain a better match between the free-space region and dielectric waveguide region.

### **Metallic Rectangular Waveguide to Ribbon Dielectric Waveguide Transition**

The ribbon transition is tailor-made for the ultra-low-loss ribbon dielectric waveguide for millimeter/submillimeter wavelengths. Figure 3 shows the transition region between a metallic rectangular waveguide supporting the dominant  $TE_{01}$  mode and a dielectric ribbon waveguide supporting the dominant

$eHE_{11}$  mode.<sup>1</sup> A flared metallic horn is used to provide the wide width for the ribbon transition region.

### **Microstripline-to-Ribbon Dielectric Waveguide Transition**

Another important, practical transition is between **microstripline**<sup>9</sup> and the ribbon dielectric waveguide. Figure 4 is a sketch of such a transition. In order to minimize **Fresnel-type** reflection losses and to accommodate the wide width of the ribbon transition, an additional transition section is added as shown. In the added transition region, it is necessary to taper the **microstripline** dielectric filling to a **vanishingly** thin wedge while the upper conducting strip is flared to a wide width. It is seen that the field concentrated under the narrow upper conducting strip of the **microstripline** is spread out through the added transition region to cover the wider width of the ribbon transition.

### **Transition for a Round Dielectric Waveguide or Fiber**

If it is desired to excite propagating fields on a round (circular) dielectric waveguide or fiber, the transition region, as shown in Fig. 5, can be designed. Here, the circular core is flared in one transverse direction and compressed in the other transverse direction into a flat ribbon and then tapered to a very narrow wedge. Again, the idea is to retain the largest possible surface area to capture the guided fields, Thus an incident plane wave can easily be captured smoothly by the thin-wide-wedge-shaped dielectric transition.

The same scheme can be used to couple **strip-laser**<sup>10,11</sup> to an optical fiber through the thin-wide-wedge transition as shown above.

## Analytical Foundation

Let us now provide some theoretical foundation<sup>12,13</sup> behind the above heuristic approach in our design of low-loss, efficient transitions to dielectric waveguides. The canonical problem is the study of the propagation characteristics of guided wave on a dielectric slab of thickness  $d$ , enclosed by two conducting plates as follows (see Fig. 6). Referring to Fig. 6, it is of interest to learn how a guided wave is detached from the conducting planes as “ $a$ ” (the separation of the two conducting plates) is increased. We wish to know how the guided field and its wave impedance of a parallel plate guide are affected by the presence of a very thin high-dielectric constant slab.

The guided mode of interest is the one whose electric field is polarized in the  $x$ -direction and whose electric field distribution is even in  $x$ . A propagation factor and a time-dependent factor of  $e^{-j\beta z + j\omega t}$ , where  $\beta$  is the propagation constant and  $\omega$  is the frequency of the wave, is implied and suppressed for all field components. In region (1), the field components for the mode of interest are

$$E_z^{(1)} = A_1 \sin \sqrt{k_1^2 - \beta^2} x \quad (1)$$

$$E_x^{(1)} = \frac{-j\beta A_1}{\sqrt{k_1^2 - \beta^2}} \cos \sqrt{k_1^2 - \beta^2} x \quad (2)$$

$$H_y^{(1)} = \frac{-j\omega \epsilon_1 A_1}{\sqrt{k_1^2 - \beta^2}} \cos \sqrt{k_1^2 - \beta^2} x \quad (3)$$

where  $A_1$  is an arbitrary constant and  $k_1^2 = \omega^2 \mu_0 \epsilon_1$ . In region (0), the field components are

$$E_z^{(0)} = A_0 \sin \left[ \sqrt{k_0^2 - \beta^2} \left( x - \frac{a}{2} \right) \right] \quad \text{for } \beta < k_0 \quad (4)$$

$$= A_0 \sinh \left[ \sqrt{\beta^2 - k_0^2} \left( x - \frac{a}{2} \right) \right] \quad \text{for } \beta > k_0 \quad (5)$$

$$E_x^{(0)} = \frac{-j\beta A_0}{\sqrt{k_0^2 - \beta^2}} \cos \left[ \sqrt{k_0^2 - \beta^2} \left( x - \frac{a}{2} \right) \right] \quad \text{for } \beta < k_0 \quad (6)$$

$$= \frac{-\beta A_0}{\sqrt{k_0^2 - \beta^2}} \cosh \left[ \sqrt{\beta^2 - k_0^2} \left( x - \frac{a}{2} \right) \right] \quad \text{for } \beta > k_0 \quad (7)$$

$$H_Y^{(0)} = \frac{-j\omega \epsilon_0 A_0}{\sqrt{k_0^2 - \beta^2}} \cos \left[ \sqrt{k_0^2 - \beta^2} \left( x - \frac{a}{2} \right) \right] \quad \text{for } \beta < k_0 \quad (8)$$

$$= \frac{-\omega \epsilon_0 A_0}{\sqrt{k_0^2 - \beta^2}} \cosh \left[ \sqrt{\beta^2 - k_0^2} \left( x - \frac{a}{2} \right) \right] \quad \text{for } \beta > k_0 \quad (9)$$

where  $A_0$  is an arbitrary constant and  $k_0^2 = \omega^2 \mu_0 \epsilon_0$ . Matching the boundary conditions at  $x = d/2$  and solving for the non-trivial solution yields the dispersion relation

$$\frac{\epsilon_0}{\epsilon_1} \frac{\sqrt{k_1^2 - \beta^2}}{\sqrt{k_0^2 - \beta^2}} \tan \left[ \sqrt{k_1^2 - \beta^2} \frac{d}{2} \right] = \tan \left[ \sqrt{k_0^2 - \beta^2} \left( \frac{d}{2} - \frac{a}{2} \right) \right] \quad \text{for } (\beta < k_0). \quad (10)$$

or

$$-\frac{\epsilon_0}{\epsilon_1} \frac{\sqrt{k_1^2 - \beta^2}}{\sqrt{\beta^2 - k_0^2}} \tan \left[ \sqrt{k_1^2 - \beta^2} \frac{d}{2} \right] = \tanh \left[ \sqrt{\beta^2 - k_0^2} \left( \frac{d}{2} - \frac{a}{2} \right) \right] \quad \text{for } (k_1 > \beta > k_0). \quad (11)$$

It is seen that, if  $d \ll a$  and if  $\beta < k_0$ , the fields inside the conducting plates are basically those of a parallel plate conducting waveguide whose propagation constant is given by

$$\left(\frac{\beta a}{2}\right) \approx \sqrt{\left(k_0 \frac{a}{2}\right)^2 - \pi^2}, \quad (12)$$

with a phase velocity,  $\omega/\beta$ , faster than the speed of light in vacuum. As  $k_0 a$  becomes large and  $\beta > k_0$ , the fields are basically governed by the fields on a slab dielectric waveguide with a phase velocity slower than the speed of light in vacuum. A sketch of the transformation (or launching) of the transverse electric field for the dominant mode from an enclosed waveguide to a dielectric ribbon guide through a wedge dielectric-flared-horn transition region (which slows down the phase velocity of the wave) is shown in Fig. 7. It is seen that  $TM_1$  mode in a conducting parallel plane waveguide can be launched, smoothly, onto a flat ribbon waveguide as the dominant  $TM_0$  mode if the transition region contains a gradually tapered section of the dielectric ribbon and a gradually flared conducting plates region. Due to the thinness and wideness of the tapered dielectric ribbon, this type of transition remains effective even when the dielectric constant of the ribbon is very large.

Let us consider this transition from the impedance matching point of view. The wave impedance of  $TM_1$  mode in the parallel plane waveguide is<sup>14</sup>

$${}_p Z_{TM_1} = \frac{\beta^{(TM_1)}}{\omega \epsilon_0} \quad (13)$$

where the subscript “*p*” means parallel plate guide, and  $\beta^{(TM_1)}$  represents the propagation constant of  $TM_1$  mode, expressed as

$$\beta^{(TM_1)} = \sqrt{\omega^2 \mu \epsilon_0 - \left(\frac{2\pi}{a}\right)^2} . \quad (14)$$

Using the same definition for wave impedance as the conducting guide, for a dielectric slab guide, one has

$${}_d Z_{TM_0}^{(0),(1)} = \frac{E_x^{(0),(1)}}{H_y^{(0),(1)}} = \frac{\beta^{(TM_0)}}{\omega \epsilon_{0,1}} \quad (15)$$

where the subscript “*d*” means dielectric slab (ribbon) waveguide and subscript “ $TM_0$ ” means the dominant mode on the dielectric slab guide,  $E_x$  and  $H_y$  are, respectively, the transverse electric field and the transverse magnetic field of the  $TM_0$  mode, and the superscript (0) or (1) refers to the region outside the dielectric slab (the cladding region) or the region inside the dielectric slab (the core region). Unlike the case for an empty conducting waveguide, the wave impedance for a dielectric slab guide, defined as the ratio of transverse electric field and transverse magnetic field, depends on the region in which it applies as shown by Eq. (15), In fact,

$$\frac{{}_d Z_{TM_0}^{(0)}}{{}_d Z_{TM_0}^{(1)}} = \frac{\epsilon_1}{\epsilon_0} . \quad (16)$$

This perhaps highlights the reason why the usual tapering technique, i.e., conical tapering to a thin apex technique, does *not* work well for high-dielectric constant,

dielectric **waveguides**. The same can be said for the tapered ribbon guide, but, because the surface area for the surface wave to “cling-to” does not decrease, the surface wave can still be attached to the ribbon structure, even when the thickness of the ribbon is very small and when the dielectric constant of the ribbon is high. Another way to look at this problem is that, since most of the guided energy of a thin ribbon electric waveguide is outside the dielectric material, the wave impedance of the dielectric ribbon can be approximately represented by the “outside” wave impedance, i.e.,  $dZ_{TM_0}^{(0)} = \beta^{(TM_0)} / \omega \epsilon_0$ , which is very close to the wave impedance of the empty parallel plate waveguide, i.e.,  $pZ_{TM_1} = \beta^{(TM_1)} / \omega \epsilon_0$ , implying good impedance matching or good launching of  $TM_1$  wave from the parallel plate guide to the  $TM_0$  mode of the thin-ribbon dielectric waveguide.

## Conclusions

A semi-heuristic way to design low-loss excitation coupler for high dielectric constant, dielectric waveguide is presented. Unlike the traditional tapered-to-a-point transition region, a tapered-to-a-thin-sheet transition region is proposed. It is found that the thin sheet gives better stability for the surface wave in the transition region; thus improving the launching efficiency for wave onto a dielectric waveguide.

## References

1. C. Yeh, F. I. Shimabukuro, and J. Chu, "Dielectric Ribbon Waveguide: An Optimum Configuration for Ultra-Low-Loss **Millimeter/Submillimeter Dielectric Waveguide**," *IEEE Trans. Microwave Theory Tech.*, vol. 38, no. 6, pp. 691-702, June 1990.
2. Conference Digest, "Seventeenth International Conference on Infrared and Millimeter Waves," California Institute of Technology, Pasadena, California, December 14-17, 1992, published by Society of Photo-Optical Instrumentation Engineers.
3. T. N. Trinh, J. A. G. Malberbe, and R. Mittra, "A metal-to-dielectric waveguide transition with application to millimeter-wave integrated circuits," 1980 *IEEE-MTT-S International Microwave Symp.*, pp. 205-207, May 1980.
4. H. M. Presby and C. A. Edwards, "Near 100% Efficiency **Fibre Microlenses**," *Electronic Letters*, vol. 28, no. 6, pp. 582-584, March 12, 1992.
5. C. Yeh, *Elliptical Dielectric Waveguides*, Ph.D. Thesis, Caltech, 1962 and *Journal of Applied Physics*, vol. 33, no. 11, pp. 3235-3243, Nov. 1962.
6. A. Ishimaru, *Electromagnetic Wave Propagation, Radiation, and Scattering*, Prentice Hall, Englewood Cliffs, New Jersey, 1991.
7. R.E. Collin, *Foundations for Microwave Engineering*, New York, McGraw-Hill, pp. 237-254, 1966.
8. M. Jamil Ahmed, "Impedance Transformation Equations for Exponential, Cosine-Squared, and Parabolic Tapered Transmission Lines," *IEEE Trans. Microwave Theory Tech.*, vol. MIT-29, no. 1, pp. 67-68, January 1981.
9. K. C. Gupta, R. Garg, and I. J. Bahl, *Microstrip Lines and Slotted Lines*, Aertech House Books, Dedham, Mass., 1982.

10. A. H. Cherin, *An Introduction to Optical Fibers*, McGraw-Hill Book Co., NY, 1982.
11. H. Kressel, *Semiconductor Devices for Optical Communication*, Springer-Verlag Press, New York, NY, 1980.
12. R. E. Collin, *Field Theory of Guided Waves*, New York, McGraw-Hill, 1960.
13. S. Ramo, J. R. Whinnery, and T. Van Duzer, *Fields and Waves in Communication Electronics*, 2nd ed., New York; Wiley, 1984.
14. F. E. Borgnis and C. H. Papas, Chapter on "Electromagnetic Waveguides and Resonators," *Handbuch der Physik*, vol. XVI, pp. 285--423, Berlin, Germany, 1958.

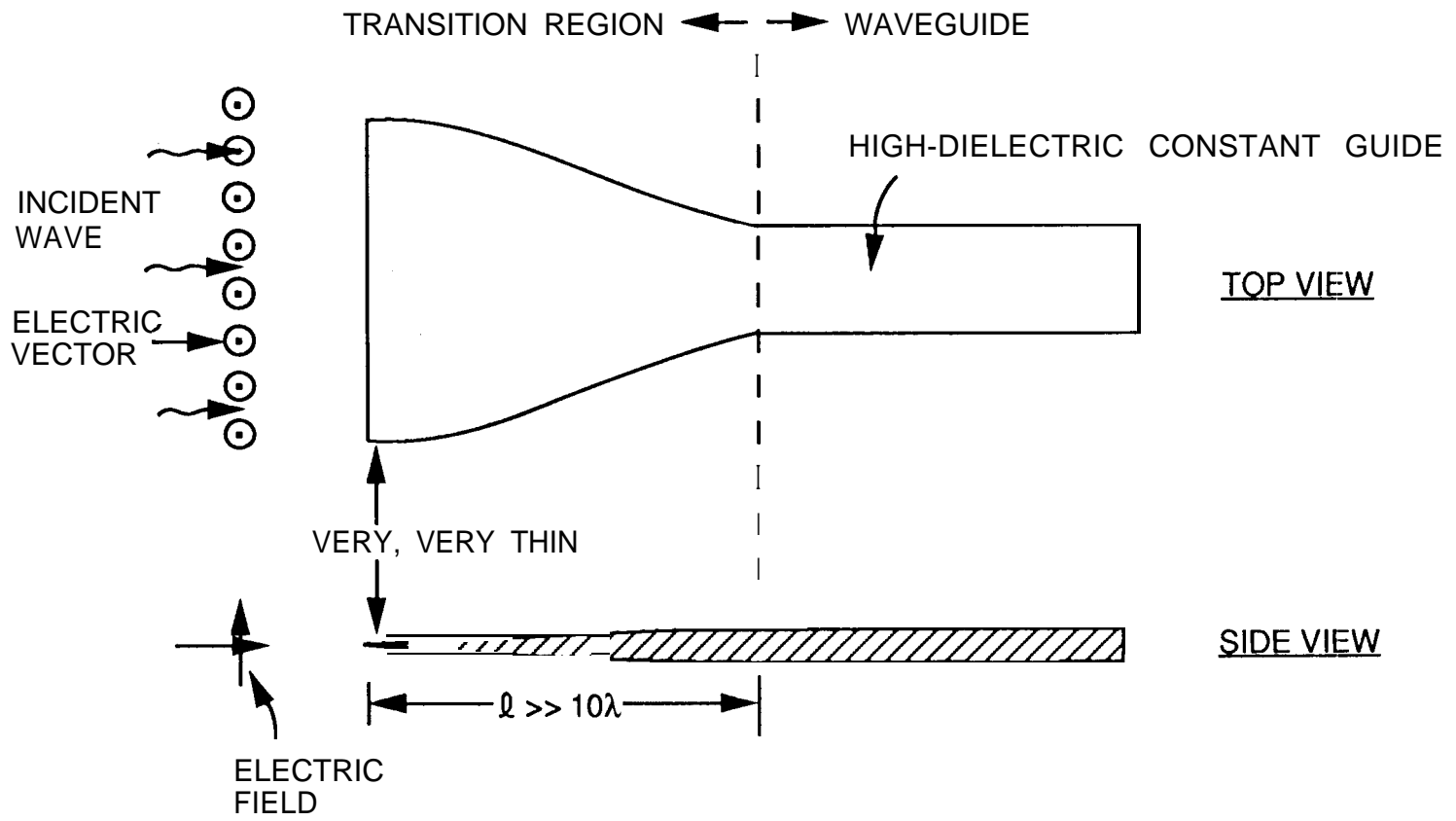


Figure 1. Tapered Section for High-Dielectric Constant Waveguide

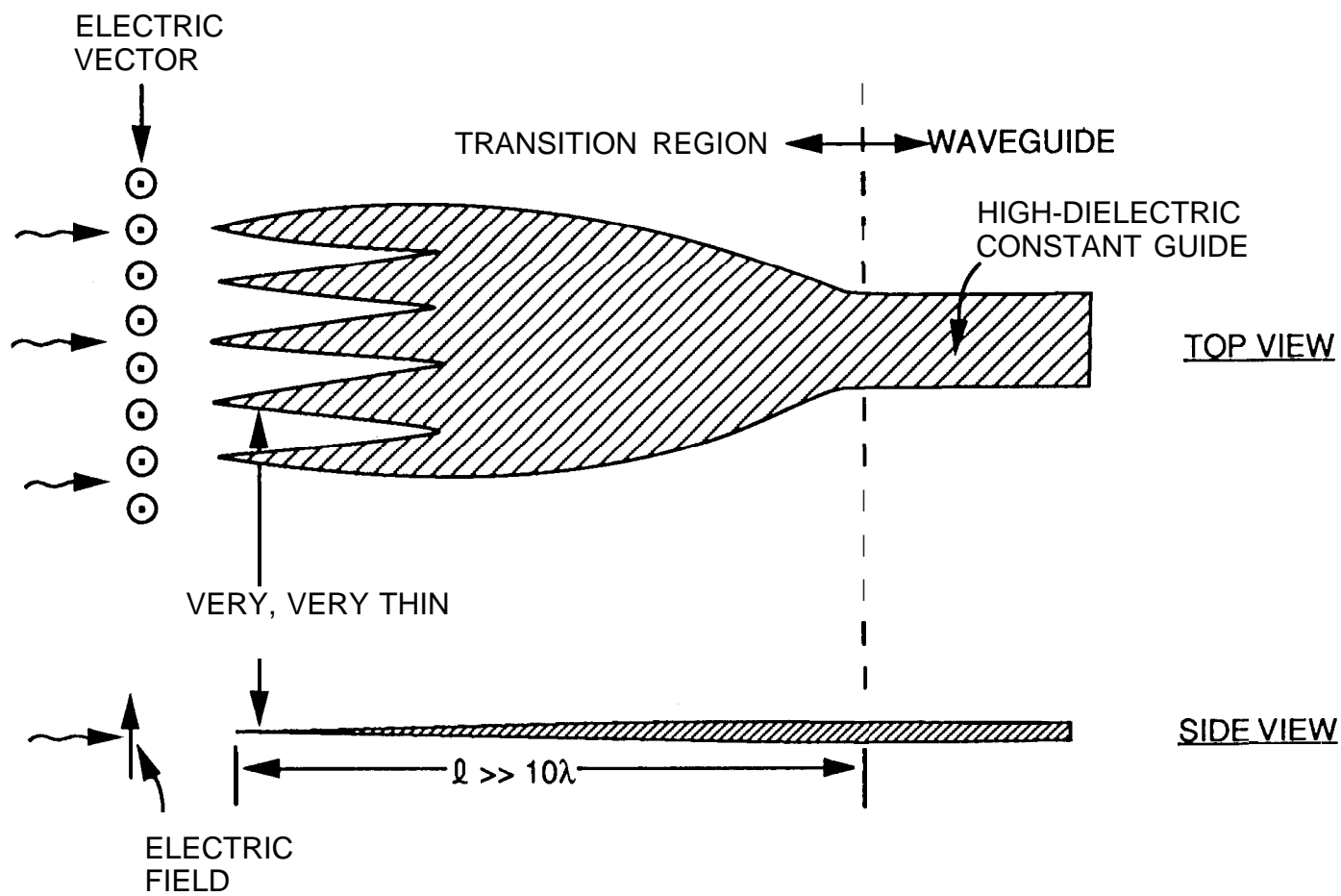


Figure 2. Comb-like Transition Region

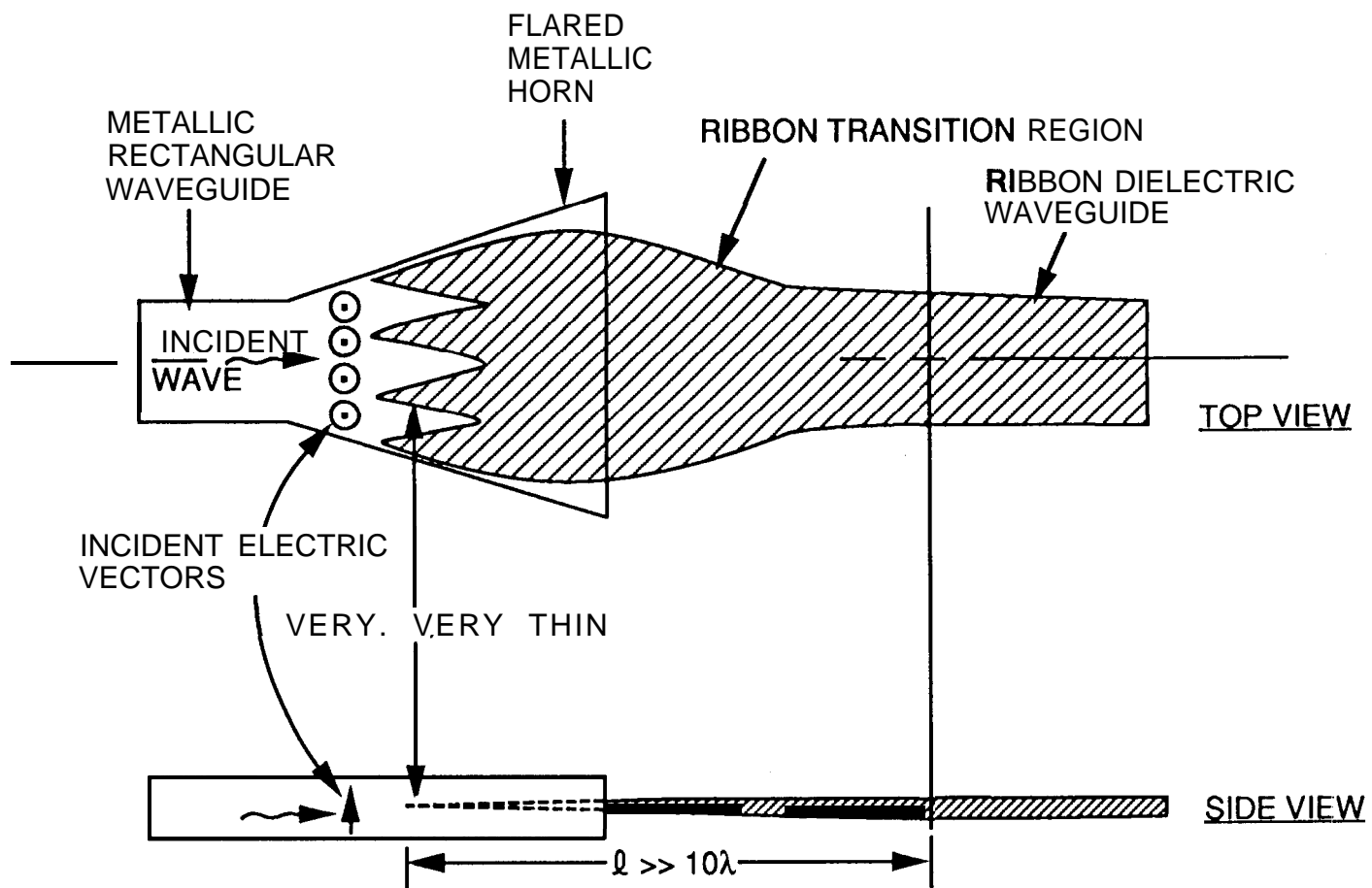


Figure 3. Metallic Rectangular Waveguide-to-Ribbon Dielectric Waveguide Transition

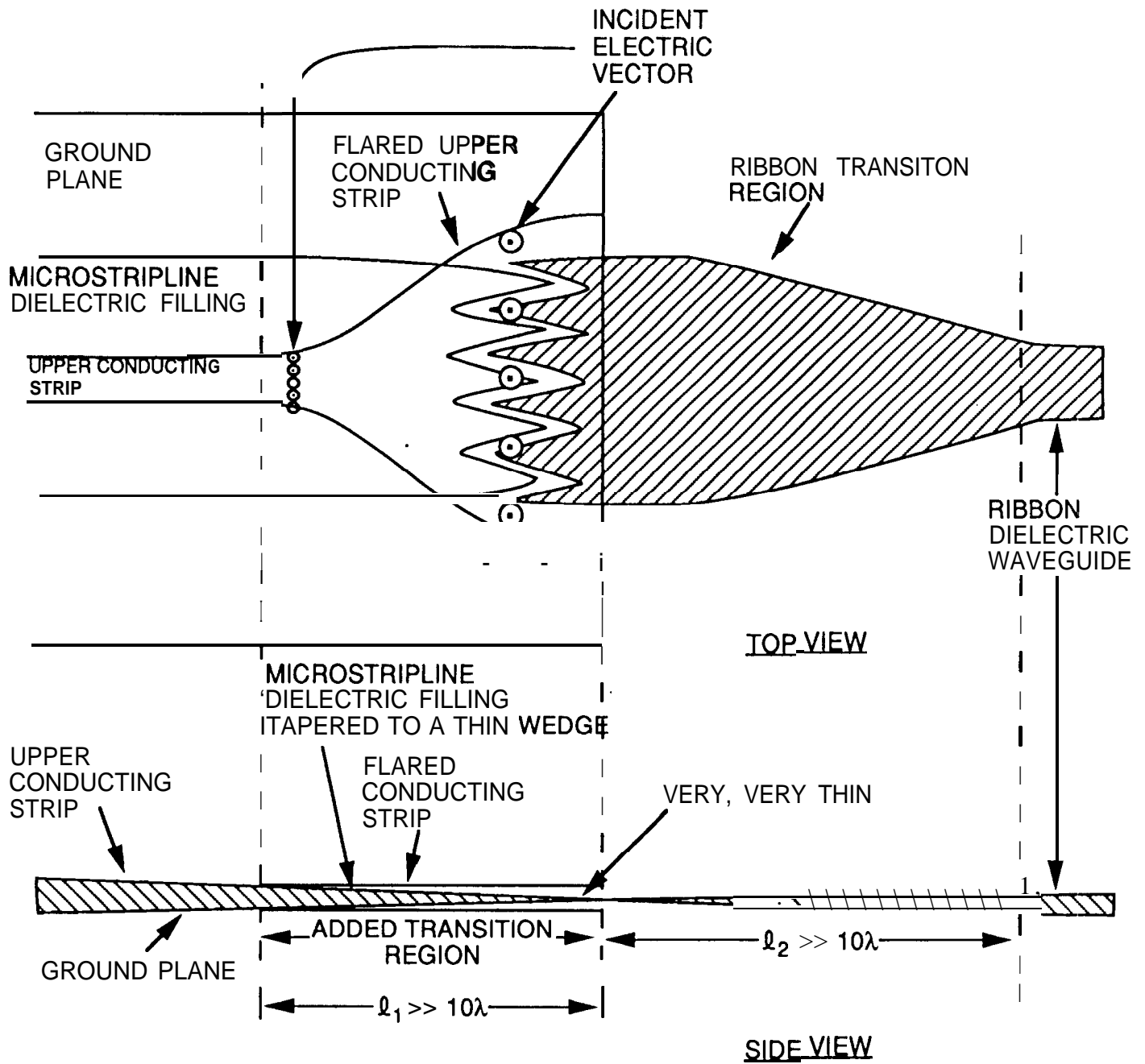


Figure 4. Microstripline-to-Ribbon Dielectric Waveguide Transition

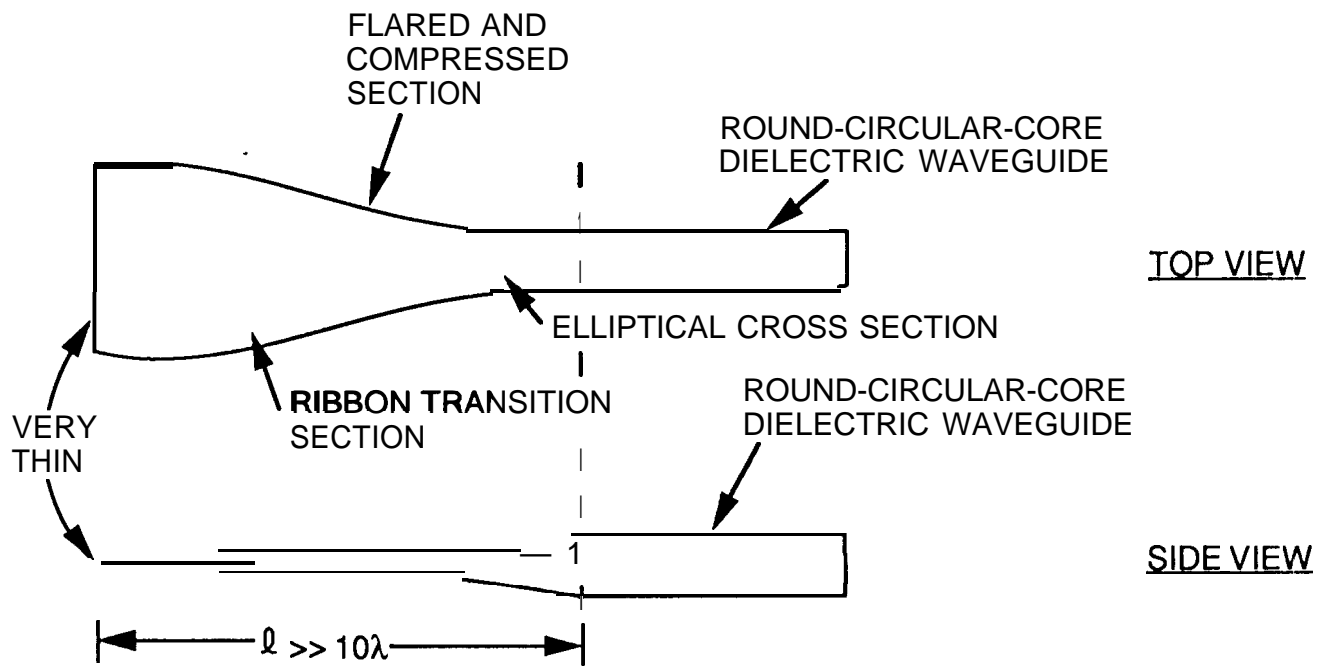


Figure 5. Transition from a Ribbon Wedge to a Round-Circular-Core Dielectric Waveguide

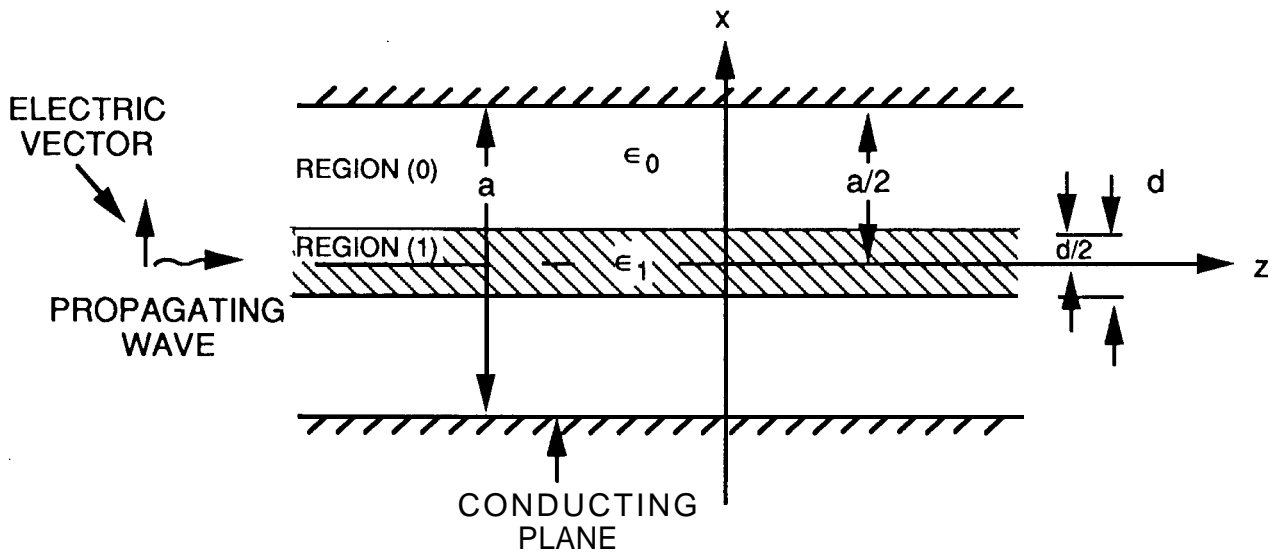


Figure 6. Geometry of the Canonical Problem

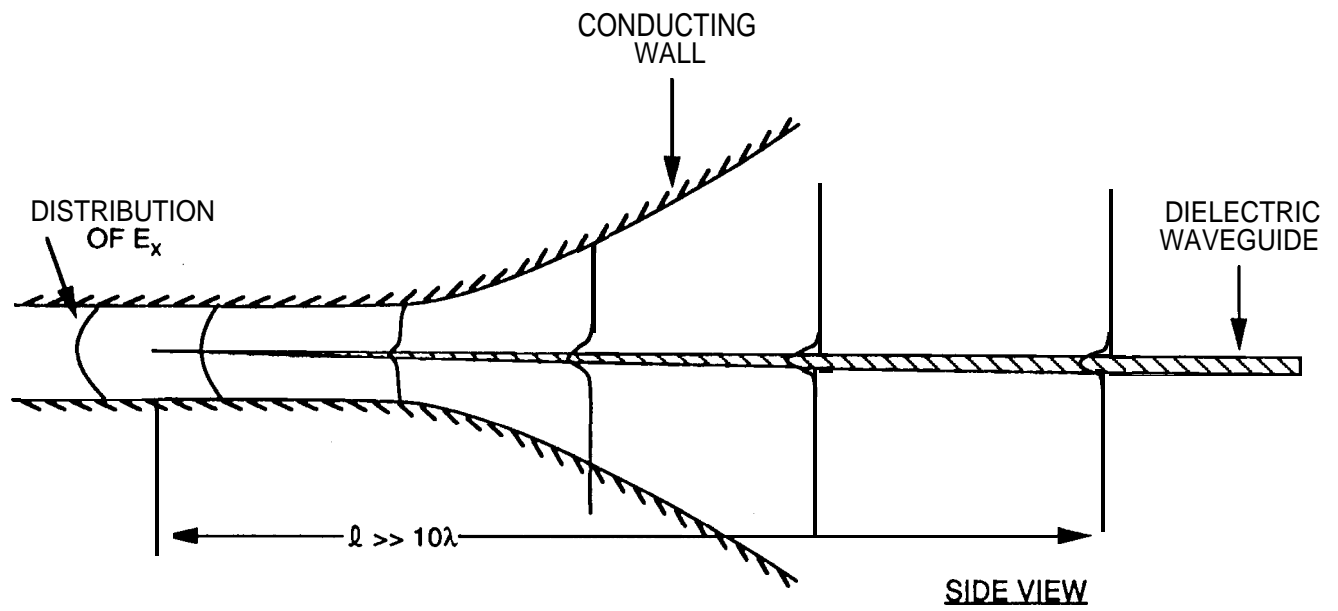


Figure 7. Transverse Electric Field Transition from an Enclosed Guide to an Open Dielectric Ribbon Guide